Oncogene (2015) **34,** 2251–2260

www.nature.com/onc

ORIGINAL ARTICLE

Deubiquitinating activity of CYLD is impaired by SUMOylation in neuroblastoma cells

T Kobayashi, KC Masoumi and R Massoumi

CYLD is a deubiquitinating (DUB) enzyme that has a pivotal role in modulating nuclear factor kappa B (NF-κB) signaling pathways by removing the lysine 63- and linear-linked ubiquitin chain from substrates such as tumor necrosis factor receptor-associated factor 2 (TRAF2) and TRAF6. Loss of CYLD activity is associated with tumorigenicity, and levels of CYLD are lost or downregulated in different types of human tumors. In the present study, we found that high CYLD expression was associated with better overall survival and relapse-free neuroblastoma patient outcome, as well as inversely correlated with the stage of neuroblastoma. Retinoic acid-mediated differentiation of neuroblastoma restored CYLD expression and promoted SUMOylation of CYLD. This posttranslational modification inhibited deubiquitinase activity of CYLD against TRAF2 and TRAF6 and facilitated NF-κB signaling. Overexpression of non-SUMOylatable mutant CYLD in neuroblastoma cells reduced retinoic acid-induced NF-κB activation and differentiation of cells, but instead promoted cell death.

Oncogene (2015) **34,** 2251–2260; doi:10.1038/onc.2014.159; published online 9 June 2014

INTRODUCTION

Neuroblastoma is the most common extracranial tumor in children, accounting for 15% of childhood cancer deaths.[1,2] Neuroblastoma originates from the sympathetic nervous system and is composed of undifferentiated and poorly differentiated neuroblasts arising from the different stages of sympathoadrenal lineage of neural crest origin.[2–5] Earlier reports have identified that in neuroblastoma the expression of markers that are upregulated in later stages of the neuronal lineage of sympathetic nervous system differentiation, such as neurotrophic tyrosine kinase, receptor, type 1 (*NTRK1*) and growth-associated protein 43 (*GAP43*), is indicative of better prognosis.[6,7] The age of patient, genetic aberrations (*N-MYC* amplification and deletion of chromosome 11 q) and metastatic spread are important factors with regard to treatment decision and patient prognosis. The International Neuroblastoma Staging System is divided into 1–4 stage groups and stage 4 S, which has the ability to spontaneously regress.[3,8] Patients older than 1½ years with stage 4 disease have the worse prognosis, with an overall survival of $< 50\%$.[2]

Surgery, chemotherapy, radiotherapy and high-dose chemotherapy with autologous stem cell transplantation are commonly used as treatment therapy for neuroblastoma patients. In addition, terminal differentiation of neuroblastoma cells induced by retinoids is used as a current standard therapy for high-risk neuroblastomas to eliminate residual tumor cells that are resistant after intensive chemotherapy and stem cell transplantation.[1,9–11] Retinoids act on upregulating diverse sets of differentiation-related gene expression via retinoic acid receptors (RAR and RXR) such as *GAP43* and neurotrophin receptors (*TrK*).[12–14] In addition, retinoids can also downregulate the expression of certain genes such as *N-MYC*, concurrent with the arrest of cell proliferation.[11,5,16] Elucidating the mechanisms behind the differentiation of neuroblastoma cells is therefore of clinical importance.

CYLD mutation was originally discovered in patients developing familial cylindromatosis, which is a benign tumor of skin appendages.[17] Loss of CYLD expression has also been found in many different tumors;[18] however, the function of CYLD in neuroblastoma is unknown. CYLD is a deubiquitinating (DUB) enzyme that cleaves lysine 63 and linear-linked polyubiquitin chains from the substrates.[19,20] Many of the known DUB substrates for CYLD include components of nuclear factor kappa B (NF-κB) signaling such as tumor necrosis factor receptor-associated factor 2 (TRAF2), tumor necrosis factor receptor-associated factor 6 (TRAF6), NF-κB essential modifier (NEMO, also named IKKγ) and B-cell lymphoma 3,[21–24] thus affecting the downstream signaling pathway. As many reports highlight the importance of CYLD expression, the regulatory mechanism of CYLD at the protein level and its influence on cellular activity and signaling remains largely unknown.

In the present study, we were able to identify posttranslational modification of CYLD by small ubiquitin-related modifier (SUMO) upon all-*trans*-retinoic acid (ATRA)-induced neuroblastoma differentiation. This posttranslation modification resulted in reduced deubiquitinase activity of CYLD against its target substrates, including TRAF2 and TRAF6, and modification of NF-κB signaling.

RESULTS

CYLD expression is associated with clinical outcomes in neuroblastoma patients

To investigate whether CYLD expression is altered in neuroblastoma, we studied the association of CYLD levels with neuroblastoma patient outcomes. A Kaplan–Meier survival analysis using a microarray data set from 88 neuroblastoma patients[25] revealed

Translational Cancer Research, Division of Molecular Tumor Pathology, Department of Laboratory Medicine, Lund University, Lund, Sweden. Correspondence: Dr R Massoumi, Translational Cancer Research, Division of Molecular Tumor Pathology, Department of Laboratory Medicine, Lund University, Medicon Village, Building 404, A3, Scheelevagen 8, Lund 22363, Sweden.
E-mail: Ramin.Massoumi@med.lu.se
Received 4 November 2013; revised 28 March 2014; accepted 28 April 2014; published online 9 June 2014

that high CYLD expression was associated with better overall survival (Figure 1a) and relapse-free neuroblastoma patient outcomes (Figure 1b). Furthermore, the relative expression level of CYLD was inversely correlated with tumor stage using the International Neuroblastoma Staging System (Figure 1c). Oncogene *N-MYC* is often amplified in aggressive and undifferentiated neuroblastomas and its expression correlates with advanced disease.[26–28] Analysis of *N-MYC* amplification in neuroblastoma patients showed that CYLD expression was significantly lower in *N-MYC*-amplified compared with *N-MYC*-non-amplified neuroblastomas (Figure 1d). We could not find any correlation of CYLD expression with the different cellular phenotypic variants of neuroblastoma cell lines, including neuroblastic (N-type; SK-N-F1, SK-N-RA, SH-SY5Y and IMR-32) or more malignant neuroblastoma cells, the intermediate type (I-type; SK-N-BE(2)C and LA-N-2). Instead, it appeared that cell lines with the lowest expression level of CYLD tend to be either multidrug resistant or derived from a patient after therapy (Figures 1e and f).

ATRA treatment increases NF-κB activation

As we found a negative correlation between CYLD and N-MYC expression (see Figure 1d), this led us to hypothesize that CYLD expression could be regulated upon differentiation of neuroblastoma. To test this hypothesis, we treated the SK-N-BE(2)C cell line with ATRA. We chose to use the SK-N-BE(2)C cell line, as this cell line expresses low levels of CYLD (see Figures 1e and f) and is highly aggressive and multidrug resistant, but still has the capacity to differentiate into neuron-like cells in response to ATRA treatment. Figures 2a and b show ATRA-mediated cell differentiation evaluated by changes in cell morphology including neurite outgrowth and downregulation of N-MYC in SK-N-BE(2)C cells. This effect was reversible by the removal of ATRA and replacing it with dimethyl sulfoxide (DMSO) (Figure 2a; ATRA → DMSO). One of the ATRA-mediated signaling pathways is the activation of the transcription factor, NF-κB.[29–31] Consistent with these reports, the NF-κB repressor protein, inhibitor of NF-κB (IκB-α), level was decreased during ATRA-induced neuroblastoma treatment, and returned to normal levels when ATRA was replaced with DMSO (Figure 2c). This observation was supported by NF-κB luciferase assay, where an increase in κB promoter activity upon ATRA treatment compared with DMSO-treated cells was observed (Figure 2d). The ATRA-mediated NF-κB activation was transient, as after 8–10 days, we could see the downregulation of NF-κB promoter activity (Figure 2e). Prolonged stimulation with ATRA (8–10 days) also led to an increase in cell death (Figure 2f). These results suggest that short time stimulation with ATRA increases NF-κB signaling and promotes differentiation of cells, whereas prolonged ATRA stimulation reduces NF-κB activation and mediates cell death.

CYLD is SUMOylated upon ATRA treatment

Next, we investigated whether stimulation of neuroblastoma cells with ATRA can affect CYLD expression. Quantitative real-time polymerase chain reaction (qRT–PCR) and western blot analyses showed a significant upregulation of CYLD gene expression in response to ATRA, which was reversible after ATRA removal (Figures 3a and b). At the protein level, after 3–6 days, we observed a slow-migrating band in cells treated with ATRA, corresponding to a posttranslational modified form of CYLD (Figure 3b). This slow-migrating band was lost when the ATRA was removed (Figure 3c). As one of the posttranslational modifiers that promotes cellular differentiation is SUMOylation,[32,33] we studied whether ATRA can alter the overall levels of SUMOylated proteins. An increase in the total levels of SUMO1- and SUMO2/3-modified proteins in cells treated with ATRA was observed. However, this effect was reversible when the medium was replaced from ATRA to DMSO (Figure 3d). To investigate whether endogenous CYLD is SUMOylated during ATRA-induced neuroblastoma differentiation,

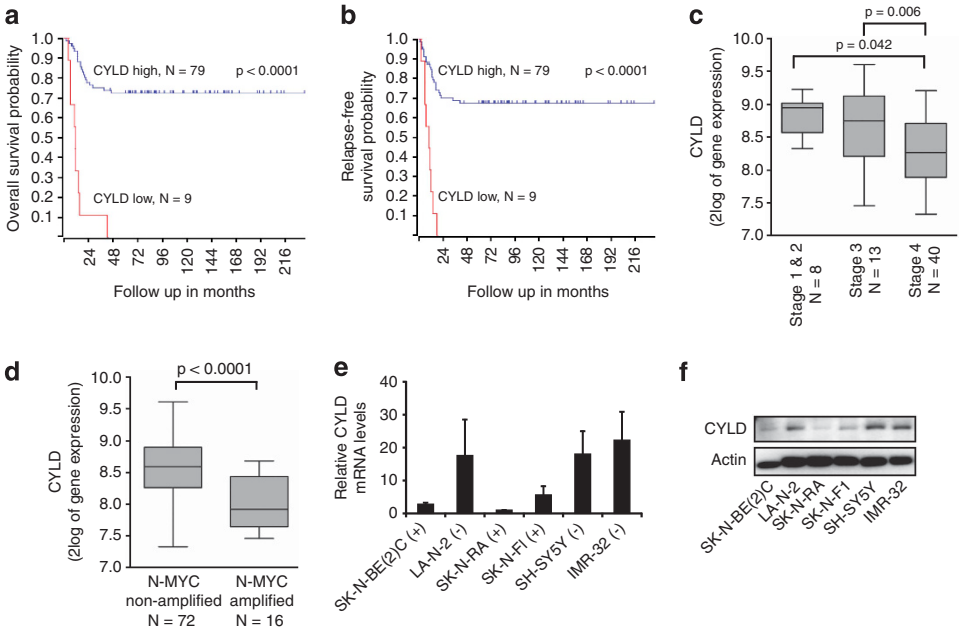

Figure 1. High CYLD expression is associated with better overall survival and is relapse-free in neuroblastoma (**a** and **b**) Kaplan–Meier survival curves for overall survival (**a**) and relapse-free survival (**b**) from 88 neuroblastoma patients (Versteeg-88-MAS5.0-u133p2) according to CYLD expression level (high or low) using the R2 microarray analysis and visualization platform (http://r2.amc.nl). Most significant expression cutoff value was used and *P*-value between two groups was calculated using a log-rank test. (**c**) Box-and-whisker plot of CYLD mRNA expression in 61 neuroblastoma patients correlated with the International Neuroblastoma Staging System that were derived from the R2 microarray analysis and visualization platform (http://r2.amc.nl). (**d**) Box-and-whisker plot of CYLD mRNA expression grouped according to *N-MYC*-non-amplified and *N-MYC*-amplified expression in 88 neuroblastoma patient samples using the R2 microarray analysis. (**e** and **f**) The levels of CYLD RNA and protein in six different neuroblastoma cell lines. (+) indicates drug resistance and (−) indicates sensitive to drug treatment.

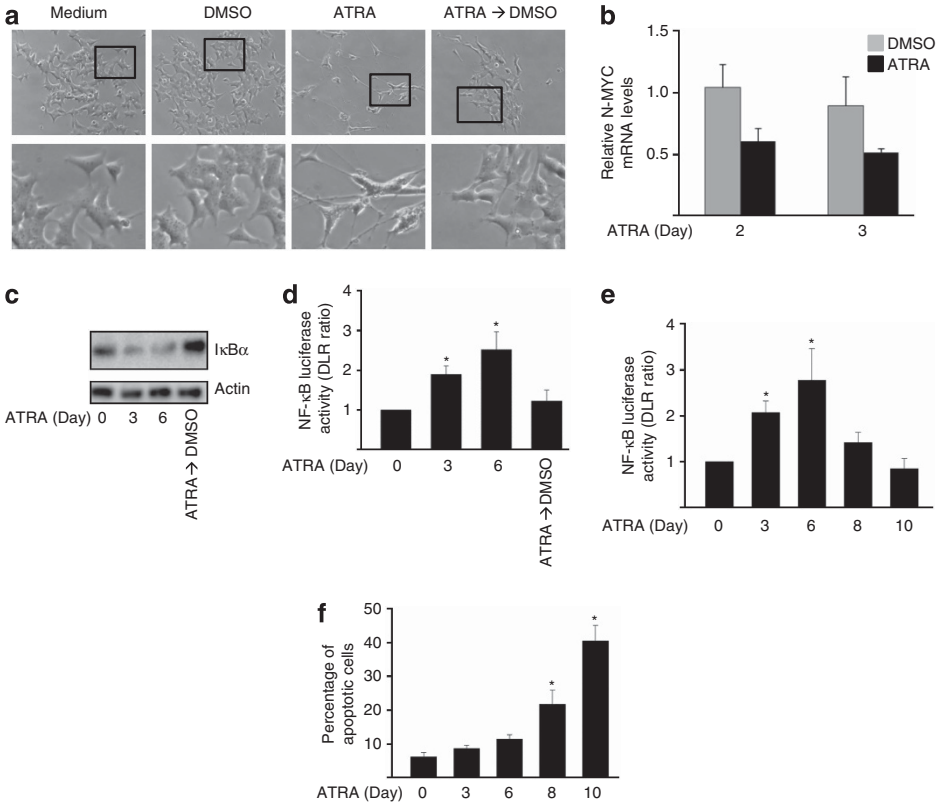

Figure 2. ATRA induces CYLD expression during neuroblastoma differentiation. (**a**) Phase-contrast microscopy images of SK-N-BE(2)C cells treated with medium, DMSO or 5 μM ATRA for 6 days. In another set of experiments, SK-N-BE(2)C cells were treated with ATRA for 3 days and ATRA was replaced with DMSO for an additional 3 days (ATRA → DMSO). Lower panel shows neurite outgrowth in cells at high magnification. (**b**) The expression of N-MYC at the mRNA level in SK-N-BE(2)C cells treated with 5 μM ATRA or DMSO for 2 or 3 days using qRT–PCR. (**c**) The levels of IκB-α in total cell lysates of SK-N-BE(2)C cells untreated or treated with 5 μM ATRA for 3 or 6 days. In another set of experiments, SK-N-BE(2)C cells were treated with ATRA for 3 days and ATRA was replaced with DMSO for an additional 3 days. (**d** and **e**) NF-κB luciferase promoter activity in SK-N-BE(2)C cells untreated or treated with 5 μM ATRA for different time points as indicated (*$P < 0.05$). (**f**) Percentage of apoptotic cells in SK-N-BE(2)C cells untreated or treated with 5 μM ATRA for 3, 6, 8 or 10 days using NucleoCounter NC-3000 (Chemometec) in conformity with the DNA fragmentation assay (*$P < 0.05$).

SK-N-BE(2)C neuroblastoma cells were treated with ATRA for 3 and 6 days and the lysates were used for immunoprecipitation with CYLD antibody. Figure 3e shows the association of SUMO with CYLD in the presence of ATRA. The reciprocal immunoprecipitation with SUMO1 or SUMO2/3 antibodies using 8 M urea-treated lysates confirmed SUMOylation of CYLD upon ATRA treatment (Figure 3f). Moreover, we found that SUMOylation of CYLD is transient. Treatment of SK-N-BE(2)C neuroblastoma cells with ATRA reduced association of SUMO with CYLD after 8 days, and SUMOylation of CYLD was completely undetected after 10 days without any changes in the total levels of CYLD (Figure 3g). The posttranslational modification of CYLD by SUMO1 and SUMO2 was further confirmed by performing *in vitro* SUMOylation assay (Figure 4a), as well as in cells overexpressing Flag-tagged full-length CYLD and SUMO1 (Figure 4b). To determine the region responsible for binding to SUMO, we generated a series of CYLD deletion mutants. As shown in Supplementary Figure 1, only CYLD 1–212 (aa 1–212) was strongly postmodified in this assay. Next, we used purified CYLD 1–212 in an *in vitro* SUMOylation assay and could show that N-terminal part of CYLD contain SUMO acceptor site (Figure 4c) for both SUMO1 and SUMO2. More specifically, lysine 40 was identified as a potential SUMO-binding site in the short fragment of CYLD protein (CYLD 1–212) using the SUMO predictor program (SUMOplot Analysis Program: http://www.abgent.com/sumoplot; Supplementary Figure S2). This sequence is highly conserved between the human, rat, mouse, bovine, chicken and chimpanzee (Supplementary Figure S3). Furthermore, mutation analysis (K40R) of this site in CYLD 1–212 (Figure 4d) or full-length CYLD construct (Figure 4e) abolished SUMOylation.

Deubiquitinase activity of CYLD is modulated by SUMOylation

Seeking an explanation for CYLD SUMOylation in ATRA-stimulated neuroblastoma cells, we analyzed stability, subcellular translocation, substrate affinity changes and DUB activity of CYLD. We could not see any differences in the stability of full-length and CYLD SUMO mutant (CYLD-K40R) by the treatment of cells with MG132, an inhibitor of 26 S proteasome-dependent protein degradation (Figure 5a). Direct visualization of EGFP-CYLD and EGFP-CYLD-K40R mutant using confocal microscopy showed that both wild-type and SUMO mutant CYLD are mainly localized in the cytoplasm of cells (Figure 5b). No differences could be observed in the substrate-binding capacity between wild-type CYLD and CYLD-K40R to TRAF2 or TRAF6 (Figure 5c). *In vitro* DUB assay demonstrated that SUMOylation of CYLD reduces DUB activity of wild-type CYLD, whereas non-SUMOylable CYLD (CYLD-K40R) could deconjugate lysine 63 chains (Figure 5d). Furthermore, the DUB activity of wild-type CYLD toward TRAF6 ubiquitination was reduced when the cells were coexpressing His-SUMO1 or His-SUMO2 (Figures 5e and f). However, coexpression of non-SUMOylable full-length CYLD (CYLD-K40R) and SUMO reduced lysine 63-linked polyubiquitin conjugation to TRAF6 (Figures 5e and f). This effect was not limited to TRAF6, as deconjugation of ubiquitin chains from TRAF2 was also dependent on the CYLD

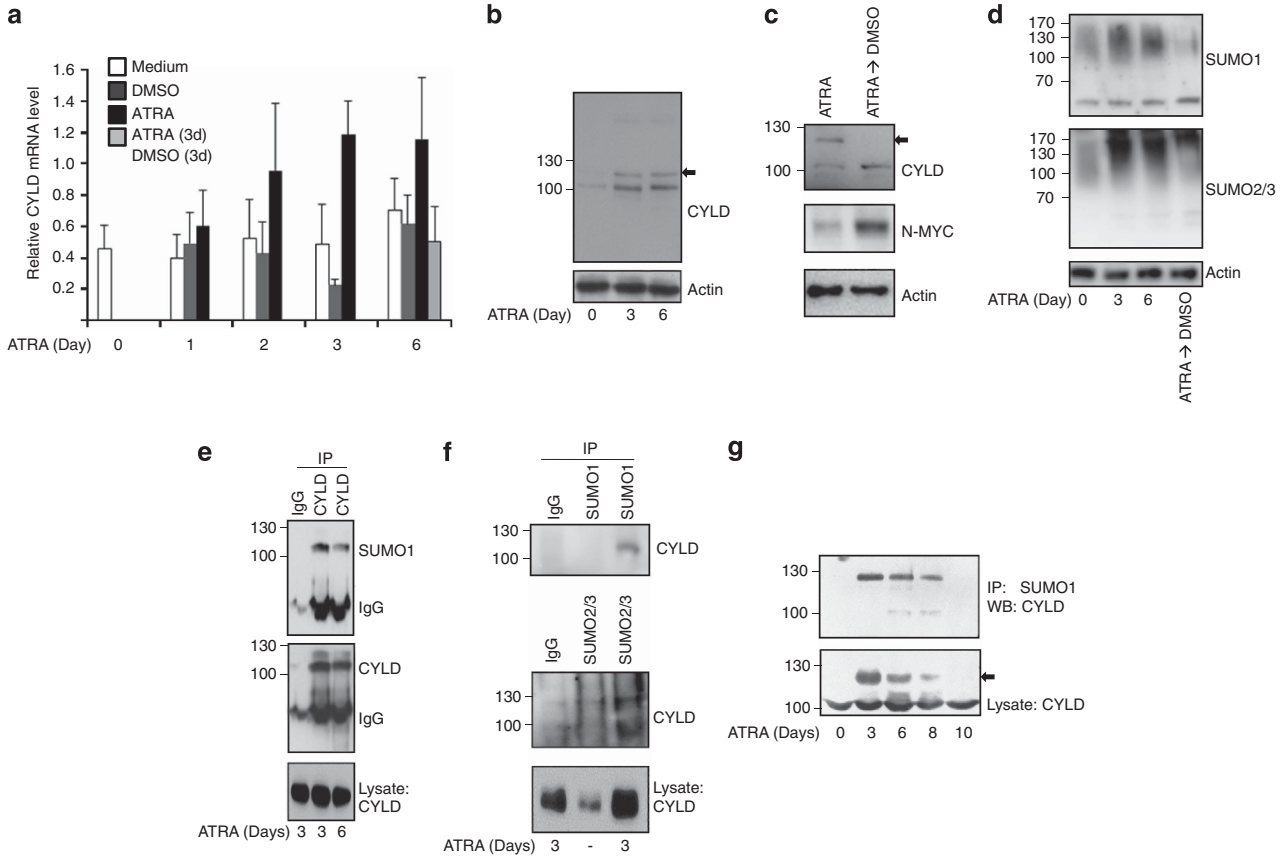

Figure 3. Posttranslational modification of CYLD induced by ATRA treatment in neuroblastoma cells. (**a**) CYLD gene expression using qRT–PCR in SK-N-BE(2)C cells in the presence of the medium, DMSO or 5 μM ATRA for 0, 1, 2, 3 and 6 days. In another set of experiments, cells were treated with ATRA for 3 days and ATRA was replaced with DMSO for an additional 3 days. (**b** and **c**) Analysis of CYLD protein expression in untreated, ATRA-treated or SK-N-BE(2)C cells treated with ATRA for 3 days and replaced with DMSO for additional 3 days. Arrowhead indicates additional slow-migrating band in ATRA-treated cells. (**d**) The levels of SUMO1 and SUMO2/3 in SK-N-BE(2)C cells untreated or treated with 5 μM ATRA for 3 and 6 days, or in cells where ATRA was replaced with DMSO for 3 days. (**e**) Endogenous immunoprecipitation (IP) of CYLD in total cell lysates from ATRA- (5 μM) treated (3 or 6 days) SK-N-BE(2)C cells, and a western blot (WB), using CYLD or SUMO1 antibodies. (**f**) Endogenous IP of SUMO1 or SUMO2/3 in 8 M urea-treated cell lysates from untreated or ATRA- (5 μM for 3 days) treated SK-N-BE(2)C cells, and a WB, using CYLD antibodies. (**g**) Endogenous IP of SUMO1 in 8 M urea-treated cell lysates from untreated or ATRA- (5 μM for 3, 6, 8 and 10 days) treated SK-N-BE(2)C cells, and a WB, using CYLD antibodies. Lower panel shows posttranslational modification of CYLD in total cell lysate of ATRA-treated SK-N-BE(2)C cells. Arrowhead indicates additional slow-migrating band in ATRA-treated cells.

SUMOylation (Figure 5g). To further confirm that the DUB activity of CYLD against its substrates is reduced because of SUMOylation, cells were transfected with TRAF2, full-length or CYLD-K40R and ubiquitin in the presence or absence of SUMO constructs. Figure 5h shows that in the absence of SUMO (lanes 5 and 7), the effect of overexpression of wild-type CYLD and CYLD-K40R on cleavage of the lysine 63-linked ubiquitin of TRAF2 was similar (Figure 5h). However, expression of SUMO together with wild-type CYLD prevented deubiquitination of TRAF2 to the same levels as in the control (lanes 3 and 4). In contrast, CYLD-K40R unconjugated ubiquitin from TRAF2, both in the presence and absence of SUMO construct (lanes 6 and 7). These results suggest that deubiquitin activation of CYLD is modulated by SUMOylation.

To test the effect of CYLD SUMOylation in ATRA-mediated NF-κB activation, we transfected SK-N-BE(2)C neuroblastoma cells with wild-type and CYLD-K40R and performed NF-κB promoter luciferase activity. CYLD-K40R mutant significantly reduced ATRA-induced κB promoter activity (Figure 5i), as well as degradation of IκB-α and phosphorylation of p65 (Figure 5j). As expected, overexpression of wild-type CYLD and CYLD-K40R reduced NF-κB promoter activity, degradation of IκB-α and phosphorylation of p65 compared with mock-transfected cells in the absence of ATRA treatment (Supplementary Figure S4). The morphologic effects of the overexpression of CYLD or CYLD-K40R in the presence of ATRA for 1 h were quantified by counting the number of transfected cells with cell processes longer than the length of two cell bodies as an indication of differentiation. In SK-N-BE(2)C cells, overexpression of CYLD induced long processes in 61% of the transfected cells, a substantially higher number than cells expressing EGFP only, where 25% of transfected cells had long processes. Expression of CYLD-K40R resulted in a decreased number of cells with long processes (35%; Figure 5k and Supplementary Figure S5). Taken together, these results suggest that SUMOylation of CYLD at lysine 40 interferes with CYLD DUB activity without any alteration in the stability, subcellular translocation or substrate affinity changes. Furthermore, SUMOylation of CYLD in neuroblastoma mediated by ATRA induces NF-κB activation and differentiation via inhibition of CYLD DUB activity (see Figure 5i).

To investigate whether CYLD expression can be correlated with differentiation markers, we used a data set from 88 neuroblastoma patients and compared CYLD expression with late sympathetic neuronal differentiation and early neural crest-associated genes. As demonstrated in Figure 6 and Table 1, we found strong correlation between CYLD and late sympathetic neuronal differentiation marker genes, such as *NTRK1*, *GAP43*, *NPY*,

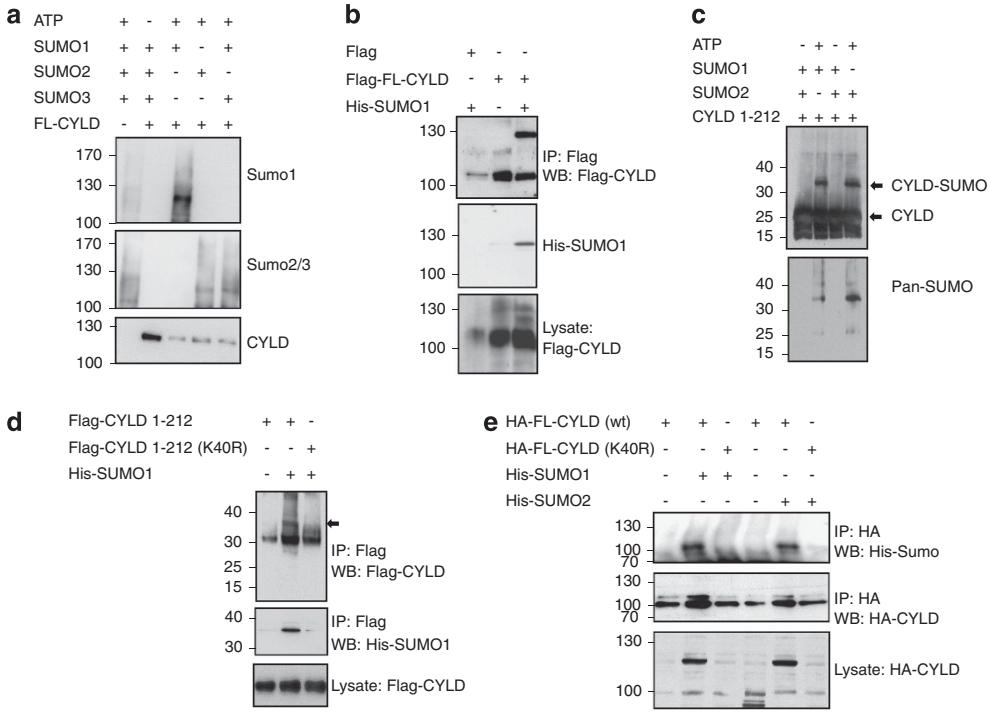

Figure 4. Identification of a SUMO conjugation motif at the N-terminal site of CYLD protein. (**a**) Purified GST-CYLD was used as substrate to perform the *in vitro* SUMOylation assay containing the E1, E2, E3 and SUMO1. Samples were immunoblotted with anti-GST, anti-SUMO1 and anti-SUMO2/3 antibodies. (**b**) Immunoprecipitation of Flag in total HeLa cell lysates transfected with Flag-tagged full-length CYLD and His-tagged SUMO1, followed by a western blot (WB), using Flag or His antibodies. (**c**) GST pull-down assay using GST-tagged short fragment of CYLD (GST-CYLD-1–222) and His-tagged SUMO1 or His-tagged SUMO2. Samples were immunoblotted with anti-GST or anti-pan SUMO antibodies. (**d**) Immunoprecipitation (IP) assay using Flag in HeLa cells transfected with Flag-tagged short fragment of wild-type CYLD (Flag-CYLD-1–222) or Flag-tagged short fragment of CYLD SUMO mutant (Flag-CYLD-K40R) and His-SUMO1 expression constructs. (**f**) IP assay using hemagglutinin (HA) in HeLa cells transfected with HA-tagged full-length CYLD constructs (wild type or mutant), His-SUMO1 or His-SUMO2 expression constructs, followed by a WB, using HA or His antibodies.

STMN2 and B-cell CLL/lymphoma *2* (Figure 6a and Table 1), whereas two of the early neural crest-associated genes, vimentin (*VIM*) and inhibitor of DNA binding 2 (*ID2*), were inversely correlated with CYLD expression (Figure 6b and Table 1).

DISCUSSION

Neuroblastoma is a rare childhood cancer that arises from the developing sympathetic nervous system. Many factors including age and stage, as well as the genetic features of the tumor, determine whether it will spontaneously regress or metastasize and become refractory to therapy. There are multiple studies defining the role of different tumor suppressor genes in the development or progression of neuroblastoma.[34] In the present study, we investigated the role of deubiquitination enzyme CYLD in neuroblastomas. Initially, we found that higher CYLD expression in neuroblastoma patient samples correlated with better survival and lower tumor stages. Furthermore, CYLD expression was significantly lower in *N-MYC* amplified, which are prediction markers for poor outcomes in neuroblastoma.[27] In addition, low CYLD expression was observed in a subset of neuroblastoma cell lines that are multidrug resistant or derived from relapsed neuroblastoma after intensive chemotherapy. Recently, ATRA has been included to the standard of care for high-risk neuroblastoma.[35] Consistent with our findings that *N-MYC*-non-amplified patients have significantly higher CYLD expression, ATRA rescues the levels of CYLD in neuroblastoma through the gene transcription mechanism. Furthermore, analyzing microarray data from neuroblastoma patient samples showed that CYLD expression was positively correlated with gene expression of late differentiation markers, including *STMN2*, *SCG2*, *NTRK1*, *BCL2* and *GAP43*, while neural crest marker genes, including *VIM* and *ID2*, were negatively correlated with CYLD expression. In general, the expression of markers that are expressed in later stages of differentiation is an indication of better prognosis.[11,17]

Previous studies identified SUMO to have a vital role in cell differentiation. Gene encoding proteins involved in SUMOylation are upregulated during Ca^{2+}-induced human keratinocyte cell differentiation and in ATRA-induced acute promyelocytic leukemia cell differentiation.[32,33] In the present study, we found that ATRA treatment of neuroblastoma cell lines leads to a transient increase in the expression of SUMO1 and SUMO2 proteins. In addition, ATRA also promoted a transient activation of the classical NF-κB signaling pathway including IκB-α degradation, phosphorylation of p65 and NF-κB promoter activity. The highest activation of NF-κB signaling and neurite outgrowth, which is a sign of neuroblastoma cell differentiation, could be observed between 1 and 6 days treatment with ATRA. Prolonged stimulation with ATRA (after 6 days) reduced NF-κB signaling and instead facilitated cell death.

ATRA-mediated upregulation of CYLD at the protein level was followed by an immediate posttranslational modification of CYLD through the SUMOylation process. However, this effect was transient. Constant CYLD SUMOylation was observed only between 1 and 6 days, whereas after 8–10 days, as the total level of CYLD protein was unchanged, the SUMOylation of CYLD was reduced. As no changes in protein stability, substrate binding or localization of CYLD SUMO mutant compared with wild-type CYLD could be observed, reduced DUB activity was identified. As transient CYLD SUMOylation paralleled NF-κB activation, we investigated whether this posttranslational modification could interfere with the NF-κB signaling pathway in ATRA-stimulated

neuroblastoma cells. Ubiquitination of TRAF2 and/or TRAF6 is an essential process for NF-κB activation, and direct binding and deubiquitination of TRAF2/6 by CYLD attenuates downstream signaling.[36,37] Here, we could show that SUMOylation of CYLD at lysine 40 prevents removal of the lysine 63-linked polyubiquitin chain from its substrates including TRAF6 and TRAF2. Furthermore,

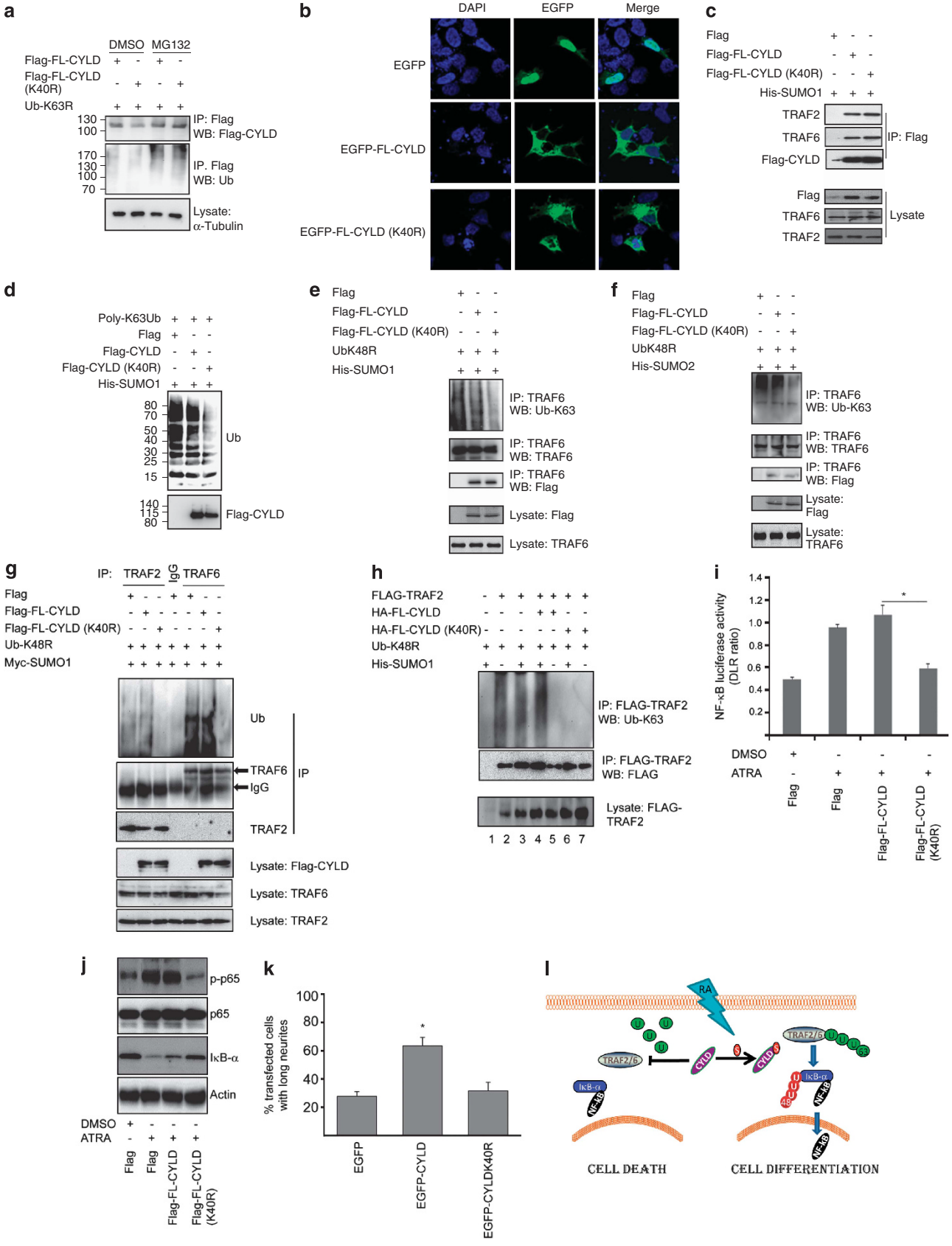

inhibition of CYLD deubiquitinase activity was essential for ATRA-mediated NF-κB signaling and differentiation of neuroblastoma cells, whereas prolonged ATRA treatment led to reduced CYLD SUMOylation, which, in turn, prevented NF-κB signaling pathway and promoted cell death. This finding suggests that the balance between non-SUMOylated and SUMOylated CYLD can direct differentiation or cell death by regulating NF-κB signaling in neuroblastoma (see Figure 5i). Indeed, retinoic acid can induce differentiation and apoptosis of neuroblastoma cells.[38,39] Previously, it has been shown that CYLD promotes apoptosis or necrosis by blocking NF-κB signaling activity.[24,40,41] In addition, the NF-κB pathway is generally tightly regulated with a negative feedback loop, for instance, by the induction of SUMO protease SENP2 upon genotoxic stress to attenuate cell survival response.[42] This raises the possibility that SUMOylation of CYLD could be reversed after initiation of neuroblastoma differentiation by negative feedback loop. This is crucial as CYLD is exclusively localized in the cytoplasm, and it has been reported that SUMOylation of extra nuclear protein can have a significant acute effect on neuronal function.[43]

In conclusion, our study provides evidence that CYLD expression in neuroblastoma is rescued by ATRA-mediated differentiation of cells and posttranslational modification of CYLD via SUMOylation. The SUMOylation of CYLD interferes with its DUB activity, which is vital for directing cell signaling decisions to promote either differentiation or apoptosis.

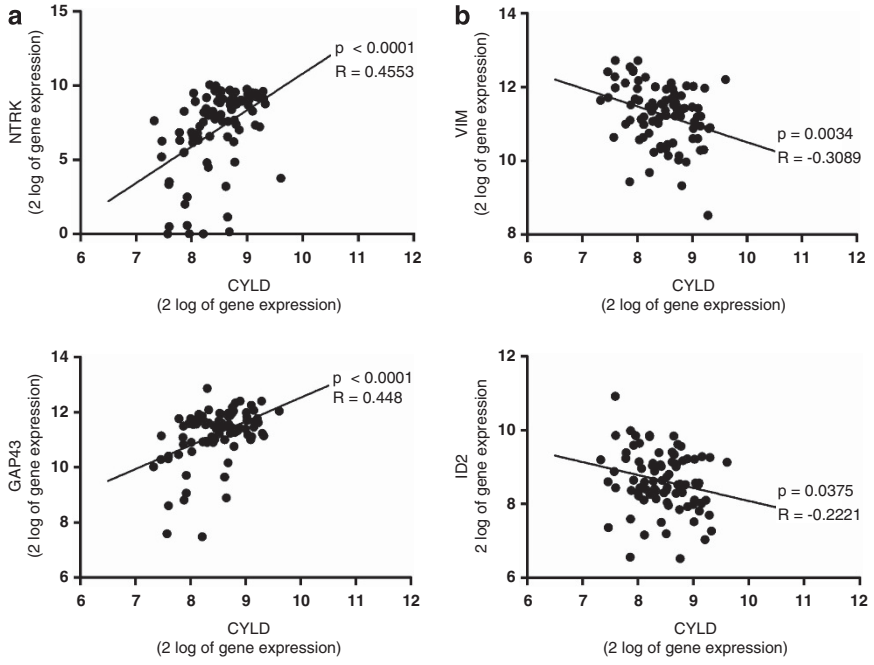

Figure 6. Correlation between CYLD and neural crest markers or late differentiation markers. (**a**) Correlation between CYLD and sympathetic neuronal differentiation marker genes (*NTRK1* and *GAP43*) were analyzed by calculating the Pearson's correlation coefficient using 88 neuroblastoma patients data extracted from the R2 microarray analysis and visualization platform (http://r2.amc.nl). Statistical analysis was carried out using two-sided unpaired *t*-test. (**b**) Correlation between CYLD and the early neural crest-associated genes (*VIM* and *ID2*) were analyzed by calculating the Pearson's correlation coefficient using 88 neuroblastoma patients data extracted from the R2 microarray analysis and visualization platform (http://r2.amc.nl). Statistical analysis was carried out using two-sided unpaired *t*-test.

Figure 5. CYLD SUMOylation reduces its deubiquitinase activity. (**a**) Western blot (WB) analysis of Flag-tagged full-length CYLD constructs (wild type or mutant) in the absence or presence of MG132 in SK-N-BE(2)C cells transfected with ubiquitin K48R, full-length or CYLD mutant constructs. (**b**) Localization of CYLD (green) and α-tubulin (red) in SK-N-BE(2)C cells transfected with EGFP, EGFP-CYLD wild-type or EGFP-CYLD-K40R, using confocal immunofluorescence microscopy. 4′,6-Diamidino-2-phenylindole (DAPI) (blue) was used for nuclear staining. (**c**) Immunoprecipitation (IP) assay using Flag in SK-N-BE(2)C cells transfected with Flag-tagged full-length CYLD (wild type or mutant) and His-SUMO1 constructs followed by a WB, using Flag, TRAF2 or TRAF6 antibodies. (**d**) *In vitro* deubiquitination assay using ubiquitin conjugation kit (Boston Biochemistry, Cambridge, MA, USA) and addition of purified full-length or SUMO mutant CYLD in the presence of purified SUMO1. (**e** and **f**) IP of endogenous TRAF6 in SK-N-BE(2)C cells transfected with wild-type or SUMO-deficient CYLD, His-SUMO1, His-SUMO2 and ubiquitin K48R constructs, followed by a WB, using Flag, K63-ubiquitin or TRAF6 antibodies. (**g**) IP of endogenous TRAF2 or TRAF6 in SK-N-BE (2)C cells transfected with Flag-tagged CYLD (wild type and mutant), Myc-SUMO1 and ubiquitin constructs, followed by a WB, using K63-ubiquitin, TRAF2 or TRAF6 antibodies. (**h**) Analysis of TRAF2 ubiquitination in HeLa cells transfected with Flag-tagged TRAF2, ubiquitin, wild-type and SUMO mutant CYLD constructs. (**i**) NF-κB luciferase activity in SK-N-BE(2)C cells untreated or treated with 5 μM ATRA for one day after transfection with wild-type or CYLD mutant expression constructs (mean ± s.e.m., $n = 3$, $^*P < 0.05$). (**j**) WB analysis of total levels of IκB-α, total p65 and phospho-p65 (recognizes serine 536) in SK-N-BE(2)C cells untreated or treated with 5 μM ATRA for one day after transfection with wild-type or SUMO mutant CYLD constructs. (**k**) The morphologic effects of the overexpression of CYLD or CYLD-K40R in SK-N-BE(2) cells in the presence of ATRA by counting the number of transfected cells with cell processes longer than the length of two cell bodies as an indication of differentiation (mean ± s.e.m., $n = 3$, $^*P < 0.05$). (**l**) Model of ATRA-mediated regulation of NF-κB signaling by CYLD in neuroblastoma cells. SUMOylation of CYLD induced by ATRA inhibits DUB activity of CYLD and prevents the removal of lysine 63-linked polyubiquitin chain from TRAF2 and TRAF6. This leads to the activation of NF-κB signaling and differentiation of neuroblastoma cells. Prolonged ATRA treatment leads to reduced CYLD SUMOylation, which, in turn, prevents the activation of NF-κB signaling via deubiquitination of TRAF2/6 and facilitates cell death.

Table 1. Correlation between CYLD and neural crest markers or sympathetic neuronal differentiation markers

	P-*value*	R	*Gene ID*
Sympathetic neuronal differentiation markers			
NTRK1 (*TrkA*)	< 0.0001	0.455	4914
GAP43	< 0.0001	0.448	2596
NPY	0.0012	0.339	4852
STMN2 (*SCG10*)	0.00027	0.38	11 075
BCL2	0.02	0.248	596
Early neuronal differentiation markers			
VIM	0.003	−0.309	7431
ID2	0.04	−0.222	3398
MEIS1	0.19	0.14	4211
MEIS2	0.45	0.082	4212
KIT	0.05	0.21	3815

Abbreviations: BCL2, B-cell CLL/lymphoma 2; GAP43, growth-associated protein 43; ID2, inhibitor of DNA binding 2; KIT, v-kit Hardy–Zuckerman 4 feline sarcoma viral oncogene homolog; MEIS1, Meis homeobox 1; MEIS2, Meis homeobox 2; NPY, neuropeptide Y; NTRK1, neurotrophic tyrosine kinase, receptor, type 1; STMN2, stathmin-like 2; VIM, vimentin. Correlation between CYLD and sympathetic neuronal differentiation marker genes or CYLD and the early neural crest-associated genes were analyzed by calculating the Pearson's correlation coefficient using 88 neuroblastoma patients data extracted from the R2 microarray analysis and visualization platform (http://r2.amc.nl). Statistical analysis was carried out using two-sided unpaired *t*-test.

MATERIALS AND METHODS

Cell culture and neuroblastoma differentiation treatments

SK-N-BE(2)C and SH-SY5Y human neuroblastoma cells were grown in minimum essential medium (MEM) (Thermo scientific, Vastra Frolunda, Sweden), whereas LA-N-2, SK-N-RA, SK-N-F1 and IMR-32 human neuroblastoma cells were grown in RPMI 1640 medium (Sigma-Aldrich, St Louis, MO, USA). HeLa cells were kept at 37 °C in a humidified atmosphere containing 5% CO_2 and 95% air. For induction of neuroblastoma differentiation, SK-N-BE(2)C cells were cultured in MEM with 1% of fetal bovine serum, 100 IU/ml penicillin and 100 μg/μl streptomycin in the presence of 1 or 5 μM ATRA (Sigma-Aldrich) for different time points. Photomicrographs of the cell morphologies were taken with a phase-contrast microscope.

For morphologic studies at the end of transfections, cells were fixed in 4% paraformaldehyde in phosphate-buffered saline (PBS) for 10 min and mounted on microscopy slides. The transfected cells were considered to have long processes if the length of the process exceeded that of two cell bodies. At least 200 transfected cells per experiment were counted.

Immunoblotting and immunoprecipitation

For immunoprecipitation studies, cells were washed three times in ice-cold PBS and lysed on ice in a RIPA lysis buffer (150 mM NaCl, 1% Triton X-100, 50 mM Tris–HCl, pH 7.6, 5 mM EDTA, 0.1% SDS, 1% Na deoxycholate) supplemented with EDTA-free Complete protease inhibitor cocktail (Roche, GmbH, Mannheim, Germany), 2.1 mM Na_3VO_4, 0.02 mM Iodoacetamide (Sigma-Aldrich), 20 mM *N*-ethylmaleimide (Sigma-Aldrich) and 1 mM phenylmethylsulfonyl fluoride (Sigma-Aldrich), and lysates were passaged through a 23 G syringe. Lysates were cleared by centrifugation at 14 000 *g* for 10 min at 4 °C, and the supernatants were precleared two times with immunoglobulin G beads for 60 min before immunoprecipitation. The precleared lysates were incubated overnight with 1–2 μg of antibodies, followed by incubation with protein G-coupled microbeads for 30 min on rotation at 4 °C. The immune complexes were recovered by applying the lysates on μColumns placed in the magnetic field of a μMACS separator (Miltenyi Biotec Norden AB, Lund, Sweden). Following washes, the complexes were eluted with sample buffer. For denatured condition, lysates containing 8 M urea was used for lysing cells and the lysates were diluted 20 times with lysis buffer without urea before immunoprecipitation.

For the immunoblotting process, whole-cell lysates were prepared using RIPA buffer with protease inhibitors and were transferred onto the polyvinylidene difluoride membranes after being resolved by sodium dodecyl sulfate–polyacrylamide gel electrophoresis. Membranes were preincubated with 5% dried milk in PBS, followed by incubation with primary antibodies. The membranes were incubated with the following antibodies: rabbit polyclonal TRAF2 (C-20; Santa cruz, CA, USA), rabbit polyclonal TRAF6 (H-274; Santa Cruz), rabbit polyclonal hemagglutinin (Y-11; Santa Cruz), rabbit monoclonal phospho-NF-κB p65 (serine 536; Cell Signaling, Beverly, MA, USA; no. 3033), rabbit monoclonal NF-κB p65 (4764; Cell Signaling), rabbit polyclonal His (2365; Cell Signaling), rabbit monoclonal K63 linkage-specific polyubiquitin (D7A11; Cell Signaling), rabbit monoclonal CYLD (D1A10; Cell Signaling), mouse monoclonal SUMO1 (21C7; Invitrogen, Camarillo, CA, USA), rabbit polyclonal SUMO1 (PW9460; Enzo Life Sciences, Farmington, NY, USA), rabbit polyclonal SUMO2/3 (PW9465; Enzo Life Sciences), rabbit polyclonal SUMO2/3 (ab3742; Abcam, Cambridge, UK), mouse monoclonal M2 Flag (F3165; Sigma-Aldrich) and previously generated rabbit polyclonal CYLD.[22] Secondary horseradish peroxidase-conjugated antibodies were obtained from GE Healthcare (Freiburg, Germany) and antibodies conjugated to Alexa dyes from Invitrogen. Control immunoglobulin G were obtained from Abcam and goat serum used for blocking from Sigma-Aldrich. The chemiluminescence was captured with a charge-coupled device camera (Fujifilm, Tokyo, Japan).

qRT–PCR

RNA was isolated using a Perfect Pure RNA Cell and Tissue Kit (5 PRIME, Hilden, Germany) according to the manufacturer's instructions. First-strand cDNA synthesis was performed using a High-Capacity cDNA Reverse Transcription Kit (Applied Biosystems, Foster city, CA, USA) with random primers and 1–2 μg of RNA. Reaction for qRT–PCR was prepared using cDNAs with SYBR Green QPCR Master Mix (Agilent, Santa Clara, CA, USA) and qRT–PCR was performed on the Mx3005P Real-Time Thermocycler (Stratagene, La Jolla, CA, USA). The following oligonucleotides were used for the qRT–PCR: CYLD (forward): 5′-TGCCTTCCAACTCTCGTCTTG-3′; CYLD (reverse): 5′-AATCCGCTCTTCCCAGTAGG-3′; N-MYC (forward): 5′-AAGTAG AAGTCATCTTCGTCCGGGTAGAAGCAGGGCTGCA-3′; N-MYC (reverse): 5′-CG ATTTCCTCCTCTTCATCTTCCTCCTCGTCATCCTCATC-3′.

Apoptosis assay

Apoptosis was evaluated, using NucleoCounter NC-3000 (Chemometec, Lillerød, Denmark), in conformity with the DNA fragmentation assay. Concisely, cells were grown on 6-well plates, harvested by trypsinization and the trypsinized cells were pooled with the cells floating in the medium. After a short centrifugation, the supernatant was removed and the precipitated cells were washed once with PBS. After a second centrifugation, the cells were resuspended in a small volume of PBS, and the single-cell suspensions were added to ice-cold 70% ethanol for fixation. Samples were vortexed and stored for 12–24 h at − 20 °C. Ethanol-suspended cells were centrifuged and the ethanol carefully decanted. Cells were washed once with PBS and then resuspended with NucleoCounter Solution 3 (1 μg/ml 4′,6-diamidino-2-phenylindole, 0.1% Triton X-100 in PBS), followed by incubation for 5 min at 37 °C. Samples of 10 μl volume were loaded into a slide chamber (NC-slide A8), and the DNA fragmentation protocol was used according to the manufacturer's instructions (ChemoMetec).

NF-κB luciferase assay

The luciferase activity in cells transiently transfected with reporter constructs containing the kB promoter was determined using the Dual Luciferase Assay system (Promega, Madison, WI, USA). The luminescent signal was quantitated using the FLUOstar Optima Plate Reader (BMG Labtech, Varmdo, Sweden). Luciferase expression was measured in cells transfected with plasmid constructs carrying the firefly luciferase reporter gene. As an internal control, plasmid pGL4.73 (Promega), containing the *Renilla* luciferase reporter gene, was co-transfected. The transfections were performed in Opti-MEM media containing 15 μl of Polyfect Transfection Reagent (Qiagen, Valencia, CA, USA), and the cells were assayed for luciferase activity at 24 h posttransfection, using reporter plasmids.

Immunofluorescence and confocal microscopy

Cells were washed in PBS, fixed with 4% paraformaldehyde in PBS for 4 min, washed two times in PBS and thereafter permeabilized and blocked

with 5% goat serum or 5% bovine serum albumin and 0.3% Triton X-100 in PBS for 30 min. Cells were incubated with primary antibodies for 1 h. Following washes in PBS, cells were incubated with secondary Alexa Fluor 546-conjugated antibodies in PBS for 1 h, followed by extensive washes in PBS and mounting on object slides using 20 µl PVA-DABCO (9.6% polyvinyl alcohol, 24% glycerol and 2.5% 1,4-diazabicyclo[2.2.2]octane in 67 mM Tris–HCl, pH 8.0). The images were obtained using a Zeiss LSM710 confocal microscope (Zeiss, Jena, Germany).

In vitro SUMOylation assay

One microgram of 6His-tagged CYLD purchased from Ubiquigent (Dundee, UK) was used as a substrate for *in vitro* SUMOylation assay using a SUMOylation Kit (Enzo Life Sciences) according to the manufacturer's instructions. Negative control reaction was carried out in the absence of ATP. After incubating the reaction for 1 h at 30 °C, the reaction was stopped by adding 2x sample buffer. SUMOylation of the protein was detected by immunoblotting using the anti-SUMO1 and anti-SUMO2/3 antibodies (Enzo Life Sciences).

In vitro deubiquitination assay

For *in vitro* deubiquitination assay, sumoylated and non-sumoylated CYLD were obtained by immunoprecipitation using the lysate prepared from SK-N-BE(2)C cells co-transfected with Flag, Flag-CYLD or Flag-CYLD-K40R together with His-SUMO1. The immunoprecipitates were incubated with 200 ng/µl of poly-K63-ubiquitin in a reaction buffer (50 mM Tris–HCl, pH 7.5, 150 mM NaCl, 2 mM EDTA pH 8.0 and 2 mM dithiothreitol) in a total volume of 30 µl. The reactions were incubated for 2.5 h at 37 °C and the reaction was terminated by adding SDS sample buffer including dithiothreitol. The reaction products were run on a sodium dodecyl sulfate–polyacrylamide gel electrophoresis gel followed by immunoblotting.

Pull-down assay

For the pull-down assay, HeLa cells were grown in 6-well plates in the presence of 10% serum, containing DMEM-GlutaMAXTM-1. After reaching 80% confluence, the cells were transfected with 2 µg of expression plasmids for 24 h. The cells were lysed with buffer containing 50 mM Tris-HCl, 150 mM NaCl, 0.5 mM EDTA and protease inhibitors. Equal amounts of cell lysate were used for the immunoprecipitation of Flag, using anti-Flag M2 affinity gel (Sigma-Aldrich), TRAF2 (C-20; Santa Cruz), TRAF6 (H-274; Santa Cruz), hemagglutinin (Y-11; Santa Cruz), SUMO1 (PW9460; Enzo Life Sciences) or SUMO2/3 (ab3742, Abcam) antibodies and incubated overnight at 4 °C. The samples were centrifuged for 5 s at 10 000 *g*, and the supernatants were discarded. The pellets were washed three times with lysis buffer and the protein concentration was measured in the resulting supernatants. Equal amounts of protein and Ni-NTA magnetic agarose beads (Qiagen) for His pull-down, Flag-peptide for Flag pull-down or protein A/G for pulling down antibodies were added to the mixture, incubated for 2 h at 4 °C and centrifuged for 5 s at 10 000 *g*. The bead complexes were collected and denatured for 5 min at 100 °C, followed by 2 min centrifugation at 12 000 *g*. The supernatants were separated using sodium dodecyl sulfate–polyacrylamide gel electrophoresis and transferred onto polyvinylidene difluoride membranes.

Statistical analyses

Statistical analyses were performed using GraphPad Prism5 Software (GraphPad Software, San Diego, CA, USA). Results are expressed as mean ± s.e.m., or as percent. *P*-values < 0.05 were deemed statistically significant. Comparisons between groups were made using the Mann–Whitney *U*-test. A correlation analysis was performed by determining the Pearson's product–moment correlation coefficient.

CONFLICT OF INTEREST

The authors declare no conflict of interest.

ACKNOWLEDGEMENTS

The plasmid for mammalian expression of His-SUMO1, His-SUMO2 and MYC-SUMO1 plasmids were a kind gift from Dr Frauke Melchior (ZMBH, Heidelberg, Germany). Flag-TRAF2 and Flag-TRAF6 plasmids were a kind gift from Dr René Bernards (The Netherlands Cancer Institute, Amsterdam, The Netherlands). We thank Dr Ingrid Ora for her critical reading of this manuscript. This work was supported by the Swedish Cancer Foundation, the Swedish Medical Research Council, the Royal Physiographic Society in Lund, the Gunnar Nilsson Foundations, the Gyllenstiernska Krapperupps Foundations, the BioCARE and by funding from the European Research Council (ERC), under the European Union's Seventh Framework Programme for Research and Technology Development (grant agreement no. 260460, awarded to RM).

REFERENCES

1 Wagner LM, Danks MK. New therapeutic targets for the treatment of high-risk neuroblastoma. *J Cell Biochem* 2009; **107**: 46–57.
2 Maris JM. Recent advances in neuroblastoma. *N Engl J Med* 2010; **362**: 2202–2211.
3 Brodeur GM. Neuroblastoma: biological insights into a clinical enigma. *Nat Rev Cancer* 2003; **3**: 203–216.
4 Anderson DJ, Axel R. A bipotential neuroendocrine precursor whose choice of cell fate is determined by NGF and glucocorticoids. *Cell* 1986; **47**: 1079–1090.
5 Anderson DJ, Carnahan JF, Michelsohn A, Patterson PH. Antibody markers identify a common progenitor to sympathetic neurons and chromaffin cells *in vivo* and reveal the timing of commitment to neuronal differentiation in the sympathoadrenal lineage. *J Neurosci* 1991; **11**: 3507–3519.
6 Fredlund E, Ringner M, Maris JM, Pahlman S. High Myc pathway activity and low stage of neuronal differentiation associate with poor outcome in neuroblastoma. *Proc Natl Acad Sci USA* 2008; **105**: 14094–14099.
7 Kogner P, Barbany G, Dominici C, Castello MA, Raschella G, Persson H. Coexpression of messenger RNA for TRK protooncogene and low affinity nerve growth factor receptor in neuroblastoma with favorable prognosis. *Cancer Res* 1993; **53**: 2044–2050.
8 Maris JM, Hogarty MD, Bagatell R, Cohn SL. Neuroblastoma. *Lancet* 2007; **369**: 2106–2120.
9 Matthay KK, Villablanca JG, Seeger RC, Stram DO, Harris RE, Ramsay NK, *et al.* Treatment of high-risk neuroblastoma with intensive chemotherapy, radiotherapy, autologous bone marrow transplantation, and 13-*cis*-retinoic acid. *N Engl J Med* 1999; **341**: 1165–1173.
10 Matthay KK, Reynolds CP, Seeger RC, Shimada H, Adkins ES, Haas-Kogan D, *et al.* Long-term results for children with high-risk neuroblastoma treated on a randomized trial of myeloablative therapy followed by 13-*cis*-retinoic acid: a Children's Oncology Group Study. *J Clin Oncol* 2009; **27**: 1007–1013.
11 Sidell N, Altman A, Haussler MR, Seeger RC. Effects of retinoic acid (RA) on the growth and phenotypic expression of several human neuroblastoma cell lines. *Exp Cell Res* 1983; **148**: 21–30.
12 Pahlman S, Ruusala AI, Abrahamsson L, Mattsson ME, Esscher T. Retinoic acid-induced differentiation of cultured human neuroblastoma cells: a comparison with phorbolester-induced differentiation. *Cell Differ* 1984; **14**: 135–144.
13 Ortoft E, Pahlman S, Andersson G, Parrow V, Betsholtz C, Hammerling U. Human GAP-43 gene expression: multiple start sites for initiation of transcription in differentiating human neuroblastoma cells. *Mol Cell Neurosci* 1993; **4**: 549–561.
14 Kaplan DR, Matsumoto K, Lucarelli E, Thiele CJ. Induction of TrkB by retinoic acid mediates biologic responsiveness to BDNF and differentiation of human neuroblastoma cells. Eukaryotic Signal Transduction Group. *Neuron* 1993; **11**: 321–331.
15 Thiele CJ, Reynolds CP, Israel MA. Decreased expression of N-myc precedes retinoic acid-induced morphological differentiation of human neuroblastoma. *Nature* 1985; **313**: 404–406.
16 Clagett-Dame M, McNeill EM, Muley PD. Role of all-trans retinoic acid in neurite outgrowth and axonal elongation. *J Neurobiol* 2006; **66**: 739–756.
17 Bignell GR, Warren W, Seal S, Takahashi M, Rapley E, Barfoot R, *et al.* Identification of the familial cylindromatosis tumour-suppressor gene. *Nat Genet.* 2000; **25**: 160–165.
18 Massoumi R. CYLD: a deubiquitination enzyme with multiple roles in cancer. *Fut Oncol* 2011; **7**: 285–297.
19 Komander D, Lord CJ, Scheel H, Swift S, Hofmann K, Ashworth A, *et al.* The structure of the CYLD USP domain explains its specificity for Lys63-linked polyubiquitin and reveals a B box module. *Mol Cell* 2008; **29**: 451–464.
20 Komander D, Reyes-Turcu F, Licchesi JD, Odenwaelder P, Wilkinson KD, Barford D. Molecular discrimination of structurally equivalent Lys 63-linked and linear polyubiquitin chains. *EMBO Rep* 2009; **10**: 466–473.
21 Trompouki E, Hatzivassiliou E, Tsichritzis T, Farmer H, Ashworth A, Mosialos G. CYLD is a deubiquitinating enzyme that negatively regulates NF-κB activation by TNFR family members. *Nature* 2003; **424**: 793–796.
22 Massoumi R, Chmielarska K, Hennecke K, Pfeifer A, Fassler R. Cyld inhibits tumor cell proliferation by blocking Bcl-3-dependent NF-kappaB signaling. *Cell* 2006; **125**: 665–677.
23 Kovalenko A, Chable-Bessia C, Cantarella G, Israel A, Wallach D, Courtois G. The tumour suppressor CYLD negatively regulates NF-[kappa]B signalling by deubiquitination. *Nature* 2003; **424**: 801–805.

24 Brummelkamp TR, Nijman SM, Dirac AM, Bernards R. Loss of the cylindromatosis tumour suppressor inhibits apoptosis by activating NF-kappaB. *Nature* 2003; **424**: 797–801.
25 Molenaar JJ, Koster J, Zwijnenburg DA, van Sluis P, Valentijn LJ, van der Ploeg I, *et al.* Sequencing of neuroblastoma identifies chromothripsis and defects in neuritogenesis genes. *Nature* 2012; **483**: 589–593.
26 Kohl NE, Gee CE, Alt FW. Activated expression of the N-myc gene in human neuroblastomas and related tumors. *Science* 1984; **226**: 1335–1337.
27 Seeger RC, Brodeur GM, Sather H, Dalton A, Siegel SE, Wong KY, *et al.* Association of multiple copies of the N-myc oncogene with rapid progression of neuroblastomas. *N Engl J Med* 1985; **313**: 1111–1116.
28 Westermark UK, Wilhelm M, Frenzel A, Henriksson MA. The MYCN oncogene and differentiation in neuroblastoma. *Semin Cancer Biol* 2011; **21**: 256–266.
29 Feng Z, Porter AG. NF- κB/Rel proteins are required for neuronal differentiation of SH-SY5Y neuroblastoma cells. *J Biol Chem* 1999; **274**: 30341–30344.
30 Kiningham KK, Cardozo Z-A, Cook C, Cole MP, Stewart JC, Tassone M, *et al.* All-*trans*-retinoic acid induces manganese superoxide dismutase in human neuroblastoma through NF-κB. *Free Radic Biol Med* 2008; **44**: 1610–1616.
31 Bryan B, Kumar V, Stafford LJ, Cai Y, Wu G, GEFT Liu M, *et al.* Family guanine nucleotide exchange factor, regulates neurite outgrowth and dendritic spine formation. *J Biol Chem* 2004; **279**45824–45832.
32 Liu T-X, Zhang J-W, Tao J, Zhang R-B, Zhang Q-H, Zhao C-J, *et al.* Gene expression networks underlying retinoic acid–induced differentiation of acute promyelocytic leukemia cells. *Blood* 2000; **96**: 1496–1504.
33 Deyrieux AF, Rosas-Acosta G, Ozbun MA, Wilson VG. Sumoylation dynamics during keratinocyte differentiation. *J Cell Sci* 2007; **120**: 125–136.
34 Cheung NK, Dyer MA. Neuroblastoma: developmental biology, cancer genomics and immunotherapy. *Nature Rev Cancer* 2013; **13**: 397–411.
35 Bauters TG, Laureys G, Van de Velde V, Benoit Y, Robays H. Practical implications for the administration of 13-*cis* retinoic acid in pediatric oncology. *Int J Clin Pharm* 2011; **33**: 597–598.
36 Deng L, Wang C, Spencer E, Yang L, Braun A, You J, *et al.* Activation of the IκB kinase complex by TRAF6 requires a dimeric ubiquitin-conjugating enzyme complex and a unique polyubiquitin chain. *Cell* 2000; **103**: 351–361.
37 Chen J, Chen ZJ. Regulation of NF-κB by ubiquitination. *Curr Opin Immunol* 2013; **25**: 4–12.
38 Lovat PE, Irving H, Annicchiarico-Petruzzelli M, Bernassola F, Malcolm AJ, Pearson AD, *et al.* Apoptosis of N-type neuroblastoma cells after differentiation with 9-cis-retinoic acid and subsequent washout. *J Natl Cancer Inst* 1997; **89**: 446–452.
39 Celay J, Blanco I, Lazcoz P, Rotinen M, Castresana JS, Encio I. Changes in gene expression profiling of apoptotic genes in neuroblastoma cell lines upon retinoic acid treatment. *PLoS ONE* 2013; **8**: e62771.
40 O'Donnell MA, Perez-Jimenez E, Oberst A, Ng A, Massoumi R, Xavier R, *et al.* Caspase 8 inhibits programmed necrosis by processing CYLD. *Nat Cell Biol* 2011; **13**: 1437–1442.
41 Wright A, Reiley WW, Chang M, Jin W, Lee AJ, Zhang M, *et al.* Regulation of early wave of germ cell apoptosis and spermatogenesis by deubiquitinating enzyme CYLD. *Dev Cell* 2007; **13**: 705–716.
42 Lee Moon H, Mabb Angela M, Gill Grace B, Yeh Edward TH, Miyamoto S. NF-κB Induction of the SUMO protease SENP2: a negative feedback loop to attenuate cell survival response to genotoxic stress. *Mol Cell* 2011; **43**: 180–191.
43 Wilkinson KA, Nakamura Y, Henley JM. Targets and consequences of protein SUMOylation in neurons. *Brain Res Rev* 2010; **64**: 195–212.

Supplementary Information accompanies this paper on the Oncogene website (http://www.nature.com/onc)